Tree Physiology, 2024, **44**, 34–45
https://doi.org/10.1093/treephys/tpae032
Advance access publication date 5 September 2023
Research paper

Optimal carbon storage during drought

Elisa Z. Stefaniak[1,2,*], David T. Tissue[2,3], Roderick C. Dewar[4,5] and Belinda E. Medlyn[2]

[1]Biodiversity Ecology and Conservation Research Group, Biodiversity and Natural Resources Program, International Institute for Applied Systems Analysis, Schlossplatz 1, Laxenburg 2361, Austria
[2]Hawkesbury Institute for the Environment, Western Sydney University, Hawkesbury Campus, Locked Bag 1797, Penrith, New South Wales 2751, Australia
[3]Global Centre for Land-Based Innovation, Western Sydney University, Hawkesbury Campus, Locked Bag 1797, Penrith, New South Wales 2751, Australia
[4]Faculty of Science, Institute for Atmospheric and Earth System Research/Physics, University of Helsinki, P.O. Box 64, Helsinki 00014, Finland
[5]Plant Sciences Division, Research School of Biology, The Australian National University, 46 Sullivans Creek Road, Canberra, Australian Capital Territory 2601, Australia

*Corresponding author (stefaniak@iiasa.ac.at)

Handling Editor: Frida Piper

Allocation of non-structural carbohydrates to storage allows plants to maintain a carbon pool in anticipation of future stress. However, to do so, plants must forego use of the carbon for growth, creating a trade-off between storage and growth. It is possible that plants actively regulate the storage pool to maximize fitness in a stress-prone environment. Here, we attempt to identify the patterns of growth and storage that would result during drought stress under the hypothesis that plants actively regulate carbon storage. We use optimal control theory to calculate the optimal allocation to storage and utilization of stored carbon over a single drought stress period. We examine two fitness objectives representing alternative life strategies: prioritization of growth and prioritization of storage, as well as the strategies in between these extremes. We find that optimal carbon storage consists of three discrete phases: 'growth', 'storage without growth' and the 'stress' phase where there is no carbon source. This trajectory can be defined by the time point when the plant switches from growth to storage. Growth-prioritizing plants switch later and fully deplete their stored carbon over the stress period, while storage-prioritizing plants either do not grow or switch early in the drought period. The switch time almost always occurs before the soil water is depleted, meaning that growth stops before photosynthesis. We conclude that the common observation of increasing carbon storage during drought could be interpreted as an active process that optimizes plant performance during stress.

Keywords: active storage, carbon source, dynamic optimization, growth–storage trade-off, non-structural carbohydrates, optimal response.

Introduction

There is currently a very active debate in the literature as to whether plant growth is primarily source-controlled or sink-controlled (Körner 2015, Fatichi et al. 2019, Cabon et al. 2022). Source control means that the plant growth rate is determined by the availability of non-structural carbohydrates (NSCs) produced during photosynthesis, whereas sink control means that the plant growth rate is determined by environmental factors such as water availability, with a feedback to the photosynthetic rate via the size of the NSC pool. Under both scenarios, the NSC pool is assumed to play a passive role, serving merely as a buffer between source and sink.

However, there is evidence that NSC storage also plays an important role as a crucial mechanism of plant stress tolerance. Larger NSC pools are associated with improved performance (O'Brien et al. 2014), higher survival rate (Kaelke et al. 2001, Poorter and Kitajima 2007, Chuste et al. 2020, Piper et al. 2022) and faster recovery from stress (Ruehr et al. 2019). When a plant is subjected to abiotic stress such as drought, the photosynthetic carbon uptake is limited (McDowell et al. 2008, Ferner et al. 2012) and the energy required for survival and post-stress recovery must be supplied by stored NSCs (Hartmann and Trumbore 2016). Thus, an alternative hypothesis to either source or sink control is that plants actively control growth rates in order to regulate the size of the NSC pool (Wiley and Helliker 2012, Dietze et al. 2014). This hypothesis is relatively under-explored despite the increasing appreciation of the importance of NSC availability in determining plant resilience to stress (Reed and Hood 2023). Our goal in this paper was to examine the consequences of this hypothesis for the dynamics of plant growth and NSC storage during a drought stress event.

Observations of plants during drought stress frequently show that growth stops before photosynthesis does, and NSC accumulates (Ayub et al. 2011, Muller et al. 2011, Tardieu et al. 2011, Boyer 2018). These observations have been interpreted to imply a physical limitation on growth, with growth being more sensitive to turgor loss than photosynthesis (Blackman 2018, Potkay et al. 2021*a*, 2021*b*). This difference in the time courses of growth and photosynthesis then results in a passive accumulation of NSCs in the plant. However, an alternative explanation to the passive storage argument is that storage accumulation during the initial drought phase is an active strategy that evolved as a way of avoiding carbon depletion during stress, ensuring that energy reserves are available when photosynthesis stops (Wiley and Helliker 2012, Dietze et al. 2014). There is some support for this argument: for example, it has been

Received: April 21, 2023. **Accepted:** March 13, 2024

shown that the timing of carbon storage allocation during drought depends on the drought tolerance of the species. Specifically, the time between the cessation of growth and that of photosynthesis (the 'carbon safety margin') is larger for drought-tolerant than non-drought-tolerant species (Mitchell et al. 2014), leading the former to accumulate more NSCs. However, to further evaluate the active storage argument, we need to understand what dynamics of growth and NSC accumulation should be expected if plants are indeed actively regulating storage.

The basis for the active storage hypothesis is that there is a trade-off between NSC storage and plant growth that plants actively regulate. Although NSC storage is essential for surviving stress, the opportunity cost of storage can be substantial. If carbon is stored rather than allocated to increasing structural or productive biomass, the opportunity to increase light capture and photosynthetic capacity is missed (Lerdau 1992). While carbon that is stored may be used for growth at a later time, the compounding benefits of early investment in growth are not realized (Bloom et al. 1985). Conversely, growth comes with additional costs: bigger plants have larger metabolic maintenance costs (Mori et al. 2010), while faster growth is associated with less resistant plant traits, such as lower wood density (Eller et al. 2018) or leaf mass per area (Wright et al. 2004, Blumenthal et al. 2020), and therefore higher stress vulnerability (Onoda et al. 2017). Faster growth means less carbon is kept in storage (Atkinson et al. 2014), which increases the plant susceptibility during stress periods, including an increased risk of significant tissue damage (Kreuzwieser and Rennenberg 2014, Ruehr et al. 2019) and mortality (Adams et al. 2017, McDowell et al. 2022).

An optimization modelling approach can be used to predict active storage dynamics during stress based on this trade-off. Optimization modelling is based on evolutionary theory (Parker and Smith 1990) and aims to find the set of actions that maximize a fitness goal (Franklin et al. 2012). Rather than assuming a priori values for parameters that determine model behaviour, optimization modelling uses the fitness goal to compute the values of these parameters. Optimization approaches have been used to explain many observations in plant systems involving trade-offs, for example: carbon allocation to root and shoot biomass (Iwasa and Roughgarden 1984, Hilbert 1990); leaf area and nitrogen content balance (Franklin 2007); and tree investment into mutualistic fungi (Moeller and Neubert 2016). When timing is a factor, dynamic optimization modelling, especially optimal control theory (OCT, Lenhart and Workman 2007), can be used. For example, the diurnal timing of stomatal regulation has been successfully modelled using dynamic optimization of the trade-off between carbon uptake and water loss (Cowan and Farquhar 1977, Medlyn et al. 2011, Lu et al. 2016, Wolf et al. 2016). Dynamic optimization models have also addressed the trade-offs in plant carbon allocation: Chiariello and Roughgarden (1984) modelled the timing of vegetative growth and reproduction in herbaceous plants over the growing season, and Iwasa and Cohen (1989) explored carbon allocation to growth, storage and reproduction that maximized reproductive output in perennial plants. In both examples, the models show that the plant must stop growing early in the season to accumulate enough storage to maximize reproduction or survive the dormancy period. These examples show that the dynamic optimization approach is promising to gain insight into the carbon storage dynamics during drought.

A key challenge in applying optimization to explore plant behaviour is to identify the fitness target to be maximized. Optimization models commonly maximize net carbon gain, or growth (Franklin et al. 2012). The best fitness targets for plants experiencing drought may vary: prioritizing growth may prove advantageous if the drought is short term or seasonal, as the plants will have a competitive edge once wet conditions return. Conversely, prioritizing storage, particularly in unpredictable environments where the lower maintenance costs associated with growth may be more suitable and access to resources for post-drought recovery is critical, can also be a strategic choice. Consequently, we propose that, during drought, plants may opt to maximize either growth or storage as a proxy for their fitness.

In this work, we identify the optimal active storage allocation under stress by applying OCT to a simple and analytically tractable 'toy' model that incorporates only the key features of carbon allocation to storage under stress. By applying OCT to a simple model representing a plant subjected to a simple drought stress regime, the optimal dynamic allocation patterns can be calculated for a range of environmental conditions and fitness assumptions. Ultimately, the model aims to provide new insight into the controls on carbohydrate storage and its role in the co-ordination of carbon source with sink demand.

Materials and methods

In summary, a simple model of a plant is presented in which the plant is subject to a drought represented by a pool of available water, which is depleted through evapotranspiration. Then, the optimal storage allocation for the plant is found in the model. First, Pontryagin's maximization principle is used to obtain the general shape of the storage utilization trajectory (Boltyanskii et al. 1960). The following alternative fitness goals are used in the analysis: (i) maximizing storage, (ii) maximizing biomass and (iii) a general case in which a combination of storage and biomass is maximized. The model is then parameterized for *Eucalyptus tereticornis* Sm. saplings using data from a Whole-Tree Chamber experiment in which the trees were subjected to drought (Drake et al. 2019). This species is used as an example to place the results within interpretable ranges, but it is intended to represent a generic forest tree species subjected to drought conditions. The model is parameterized and the exact optimal solution is then found numerically.

Simple model

The simple model represents photosynthesis, respiration, water use and growth during a drought period (Figure 1). The plant has two carbon pools: biomass (M) and storage (S), which are increased and decreased by the biological processes of photosynthesis (A), respiration (R) and growth (G). The environment is represented by a soil water pool (W) which is reduced by evapotranspiration (E). The W is defined as the amount of water available for use by the plant. There is no water input during the drought and, therefore, the only water available to the plant is the initial available water, W_0. We use a simple, linear representation of all carbon and water processes.

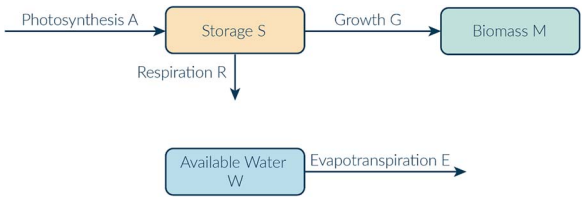

Figure 1. Conceptual model of carbon allocation in a droughted plant and its soil water availability. The model consists of two carbon pools (storage, yellow and biomass, green) and a single water pool (blue). Storage (*S*) represents available labile carbon that can be used for respiration (*R*) or growth (*G*) of the plant. Photosynthetic uptake (*A*) is first delivered to storage to later be utilized for respiration and growth of biomass. The available water pool is depleted through evapotranspiration (*E*) proportional to plant photosynthesis.

The time course of utilization of stored carbon to biomass is flexible and can be optimized, using OCT, once the fitness objective is defined.

The storage pool S consists of plant labile carbon. It is increased through photosynthesis (A) and can be used for respiration (R) or for growing new biomass (G). The rate of change of storage is:

$$\frac{dS}{dt} = A - R - G. \tag{1}$$

Plant biomass M is represented as a single undifferentiated pool and is changed only through growth:

$$\frac{dM}{dt} = G. \tag{2}$$

Photosynthesis and respiration are assumed to be directly proportional to the amount of biomass M:

$$A = k_{\mathrm{p}} M, \tag{3}$$

$$R = k_{\mathrm{r}} M, \tag{4}$$

where k_{p} and k_{r} are, respectively, the rates of photosynthesis and respiration per unit biomass.

To keep the model parsimonious, biomass growth and storage depletion are represented by a single flux, growth (G), which is determined by the amount of carbon in storage and a utilization coefficient that varies over time:

$$G = u_t S, \tag{5}$$

where u_t is the growth rate per unit of storage (storage utilization coefficient), which is a function of time (t). The value of u_t is assumed to have an upper bound given by k_s, the maximum storage utilization parameter:

$$0 \leq u_t \leq k_s. \tag{6}$$

The time course of the growth coefficient u_t is flexible and can be optimized, using OCT, once the fitness objective is defined.

The plant is modelled over a deterministic drought period of length T. As a simplifying assumption, a plant is considered to be alive only while its storage pool $S(t)$ is greater than or equal to zero. This factor, in turn, implies that the end-of-drought storage (S_{T}) must be greater than or equal to zero (further explained in Stefaniak 2021):

$$S(t) \geq 0 \Rightarrow S_{\mathrm{T}} \geq 0. \tag{7}$$

At the outset, the plant has access to a specified initial soil water pool (W_0). No additional water is supplied during the observed period and post-drought conditions are ignored. The plant consumes soil water during photosynthesis through evapotranspiration, E, at a rate of k_{w}, where k_{w} is the inverse of the water-use efficiency (Bierhuizen and Slatyer 1965, Sinclair et al. 1984):

$$\frac{dW}{dt} = -\mathrm{E} = -k_{\mathrm{w}} A. \tag{8}$$

The soil water pool is constrained within the model to always be positive:

$$W(t) \geq 0. \tag{9}$$

Photosynthesis is assumed to be dependent on the water availability. The photosynthesis parameter k_{p} is a constant when the available soil water is positive and becomes zero when $W(t)$ goes to zero:

$$k_{\mathrm{p}} = \begin{cases} 0 \text{ when } W(t) = 0 \\ k_{\mathrm{p}}^{*} \text{ when } W(t) > 0 \end{cases}. \tag{10}$$

The time at which the available water goes to zero is denoted as t_{crit}. To satisfy the plant's metabolic requirements when the plant is photosynthesizing, the photosynthetic gain must be greater than metabolic costs. This is implemented by constraining the value ofk_{p}^{*}:

$$k_{\mathrm{p}}^{*} > k_{\mathrm{r}}. \tag{11}$$

Parameter estimation

Table 1 lists the relevant parameters, with units and baseline values. Values are derived from a study by Drake et al. (2019) in which young *E. tereticornis* trees were exposed to factorial warming × rainfall reduction treatments in whole-tree chambers for 15 months. Parameters were obtained from the control treatment trees. The drought length T was set to 150 days.

Fitness objective

Evolutionary theory posits that, given sufficient time, species will evolve such that they maximize evolutionary fitness (Parker and Smith 1990), where fitness is defined as the overall reproductive success, including the survival of all offspring produced. However, because reproductive success is exceptionally challenging to estimate for long-lived species such as trees, it is common to use a proxy for fitness, such as maximizing wood production (McMurtrie and Dewar 2013). Here, because it is not clear what outcome would maximize long-term fitness, we first consider two alternative proxies

Table 1. Table of variables and parameters used in the model.

Symbol	Units	Value	Description
Carbon and water pools			
S_t	gC plant^{-1}	—	Storage carbon pool
S_0	gC plant^{-1}	550	Initial storage carbon pool
M_t	gC plant^{-1}	—	Biomass carbon pool
M_0	gC plant^{-1}	3300	Initial biomass carbon pool
W_t	kg H_2O plant^{-1}	—	Available soil water pool
W_0	kg H_2O plant^{-1}	1200	Initial soil water pool
Time parameters			
T	days	150	Simulated drought length
t_s	days	—	Time of switch from allocating carbon to biomass to allocating carbon to storage
t_{crit}	days	—	Time at which soil water pool runs out
Process parameters			
k_p	gC g^{-1}C days^{-1}	—	Photosynthesis parameter
k_p^*	gC g^{-1}C days^{-1}	0.2	Maximum value of the photosynthetic parameter
k_r	gC g^{-1}C days^{-1}	0.06	Respiration parameter
k_w	kg H_2O g^{-1}C	0.4	Water-use parameter
k_s	gC g^{-1}C days^{-1}	0.06	Maximum storage utilization parameter
u_t	gC g^{-1}C days^{-1}	—	Storage utilization rate
k_f	—	0–1	Fitness proxy parameter

for maximizing fitness: maximizing biomass (M_T; herein, MaxM) and maximizing storage (S_T; herein, MaxS) at the end of drought period T.

The MaxM proxy can be taken to represent fitness because the plant with the largest biomass at the end of the stress period can potentially outcompete its neighbours and provide increased carbon to reproduction. However, this optimization target is subject to the plant maintaining a sufficiently large storage pool such that S does not become negative, or die, during the stress period. This proxy may best represent fitness when plants experience a short stress period and rely on a continued supply of immediate carbon through photosynthesis for reproduction (sometimes referred to as 'income breeding', Stearns 1989). Maintaining a large biomass pool would increase the current assimilates that can be redirected to reproduction post-stress and enhance fitness in environments where plants experience 'predictable' (e.g., seasonal) stress and the plant can maintain a sufficiently large storage pool buffer to survive. Storing additional carbon may be detrimental to fitness when the approximate length and intensity of stress are unlikely to vary much year to year. Therefore, carbon that is not used will incur a cost to potential competitive and reproductive effort.

However, the total biomass at the end of a stress period may not represent fitness in environments that experience more intense, or uncertain, stress. The alternative fitness proxy, MaxS, can be taken to represent fitness because a large storage pool at the end of the stress period can be used to recover after the stress event and may increase the carbon available for reproductive effort following stress. Post-stress, plants can redirect stored carbon to reproduction (a strategy referred to as 'capital breeding', Stearns 1989), thus increasing their evolutionary fitness (Kozlowski 1992). However, reproduction is not explicitly included in the model, which focuses on survival during a single stress period. Increased growth can become detrimental to the plant as additional biomass will increase costs, thus decreasing storage and potential carbon for reproduction. However, while a smaller plant might have increased survival chances because of this strategy, it is less likely to perform competitively against plants with strategies maximizing their competitive output through growth. Thus, the MaxS strategy is more advantageous when the stress risk is significant enough to warrant a large storage pool and benefits to reproduction can accumulate over a lifetime.

The two alternative fitness proxies may represent fitness in different environments, but they may also be thought of as representing different life-history strategies. Variations in life-history strategies are often observed within a single environment, both in terms of individual traits and the individual position on a trade-off spectrum (Clark et al. 2007, Rüger et al. 2020). The MaxM and MaxS strategies differ in their trade-offs to stress risk, survival and overall benefits to lifetime reproduction. Hence, we can consider MaxM to be a 'risky' strategy and MaxS to be a 'safe' one.

In addition to MaxM and MaxS, we also consider fitness objectives that are linear combinations of these two objectives:

$$\Phi_{k_f} = k_f M_T + (1 - k_f) S_T, \tag{12}$$

where $k_f$is the fitness proxy parameter taking on a value between 0 and 1. MaxM and MaxS are special cases of Φ_{k_f} with $k_f = 1$ and $k_f = 0$, respectively.

The OCT solution

The approach taken here is to initially find the optimal storage utilization rate (u_t) which maximizes the final carbon pool (J; where J refers to the function being maximized). It is solved using the Pontryagin Maximum Principle (Boltyanskii et al. 1960) from OCT (Lenhart and Workman 2007, Stengel 2012). Following this method, a solution for the MaxS problem can be found (see Stefaniak 2021). The results of this analysis indicate that the behaviour of the optimal allocation trajectory follows the so-called 'bang-bang' behaviour (Lenhart and Workman 2007), where the optimal growth coefficient, u_t^*, takes on only the minimal or maximal value within the allowed bounds. The time point at which the plant switches between the maximal and minimal value of u_t^* is

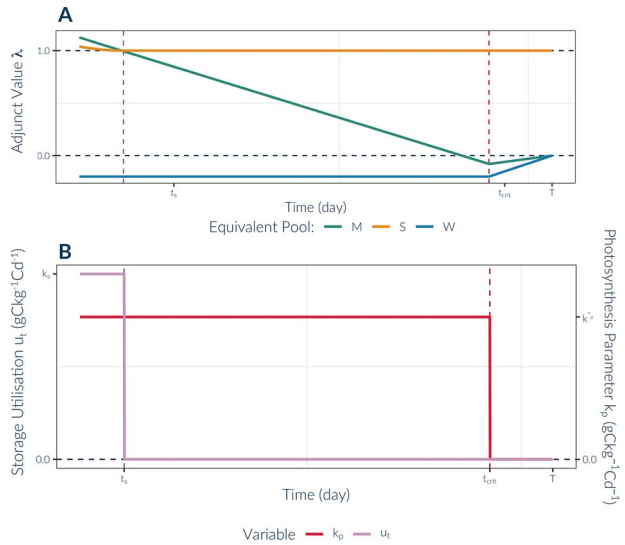

Figure 2. (A) Trajectory of the adjunct values over the three phases of optimal growth: growth, storage and stress. Each line represents an adjunct equivalent to a different pool in the model: biomass (λ_M, green), storage (λ_S, yellow) and soil water (λ_W, blue). Vertical dashed lines correspond to points at which adjunct function changes and, therefore, the phase of optimal growth changes: pink line for t_s when growth stops (switch from growth to storage phase) and red line for t_{crit} at the point at which photosynthesis stops (switch from storage to stress phase). (B) Equivalent values of the storage utilization rate u_t (pink) and the photosynthesis parameter k_p (red) throughout the three phases of optimal growth.

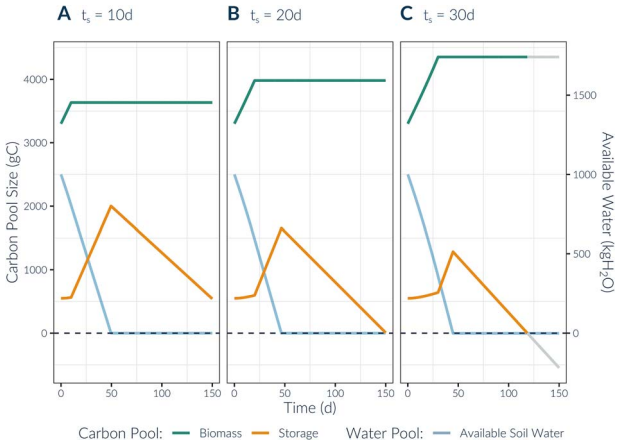

Figure 3. Carbon and water pool trajectories using different switch times (A: $t_s = 10$ days; B: $t_s = 20$ days and C: $t_s = 30$ days) and an initial water availability of $W_0 = 1000\ kgH_2O$. The biomass pool (green line) increases until the switch time and then remains constant for the rest of the simulation. The storage pool (yellow line) increases gradually before the switch time. After the switch time, it increases linearly until the point at which the water runs out. It then decreases at a constant rate until the end of the simulation. With an early switch time (A, $t_s = 10$ days), some storage remains available to the plant at the end of the simulation. A later switch time (B, $t_s = 20$ days) leads to all the stored carbon being used up. Finally, in the third case (C, $t_s = 30$ days), there is not enough storage to keep the plant alive until the end of the simulation. The plant dies once the storage is used up (grey line).

defined as the switch time, t_s. In general, there are three periods that can be distinguished in the optimal trajectory (Figure 2): growth, storage and stress:

i) Growth: $t < t_s$, $u_t^* = k_s$, $W_t > 0$
ii) Storage: $t_s < t \leq t_{crit}$, $u_t^* = 0$, $W_t > 0$
iii) Stress: $t_{crit} < t < T$, $u_t^* = 0$, $W_t = 0$

The length of each period is dependent on the specific goal function (through the fitness parameter k_f) and the initial water availability W_0. For both MaxS ($k_f = 0$) and MaxM ($k_f = 1$), there are some special cases where the optimal trajectory differs from this three-stage trajectory. For MaxS these are: (i) water is never limiting ($W_T > 0$); (ii) there is enough water for the plant to survive but not to support any growth; and (iii) initial water availability is insufficient to support the plant, and death occurs. For MaxM, there are two additional special cases: (i) water is limiting ($W_T = 0$), but growth is supported from stored carbon such that the time of water depletion (t_{crit}) and growth cessation (t_s^*) is reversed ($t_{crit} < t_s^* < T$), but a plant must still experience a storage phase; and (ii) water is limiting ($W_T = 0$), but the plant can grow throughout the entire simulation ($t_{crit} < t_s^* = T$). A full derivation of these cases along with the equations and characteristics can be found in Stefaniak (2021).

Numerical solution of optimal switch time

The analytical solution outlined above demonstrates that the optimal trajectory consists of a period of maximum growth followed by a switch to zero growth at time t_s^*. Thus, the optimal trajectory can be quantified in terms of the value of t_s^*. Here, we solve the value of t_s^* numerically using a simulation approach applied to the simplified model (Eqs. (1)–(11)). The classic Runge–Kutta method (Stengel 2012) is explicitly implemented to solve the model in continuous time using a time-step size of $\Delta t = 0.1$ days. The approach generates storage and biomass trajectories for a range of possible values of t_s (0–150 days). From these trajectories, we find the value $t_s = t_s^*$ that gives the maximum value of the goal function.

Results

Storage schedule: description of the general solution

The emergence of the two dividing time points, the time of switch to zero growth (t_s) and the time of water depletion (t_{crit}), leads to a three-phase storage utilization strategy, illustrated for three t_s values in Figure 3. In the first phase ($0 < t < t_s$), i.e., the growth period, the plant uses a proportion of the storage it has available to growing its biomass, thus increasing subsequent photosynthate production (A). During this time, biomass and storage grow exponentially, while water is being used up at an increasing rate as the biomass growth leads to exponential water loss. During the second stage ($t_s < t < t_{crit}$), the storage period, the growth rate is zero. Respiration costs are continuous throughout this period but are smaller than photosynthetic uptake, leading to a linear increase in storage. The available water also decreases linearly. At $t = t_{crit}$, the water runs out and photosynthesis stops. For the remainder of the simulation ($t_{crit} < t < T$), the stress period, the plant must support its respiration requirement by drawing on any stored carbon. The storage pool decreases linearly for the remainder of the simulated period.

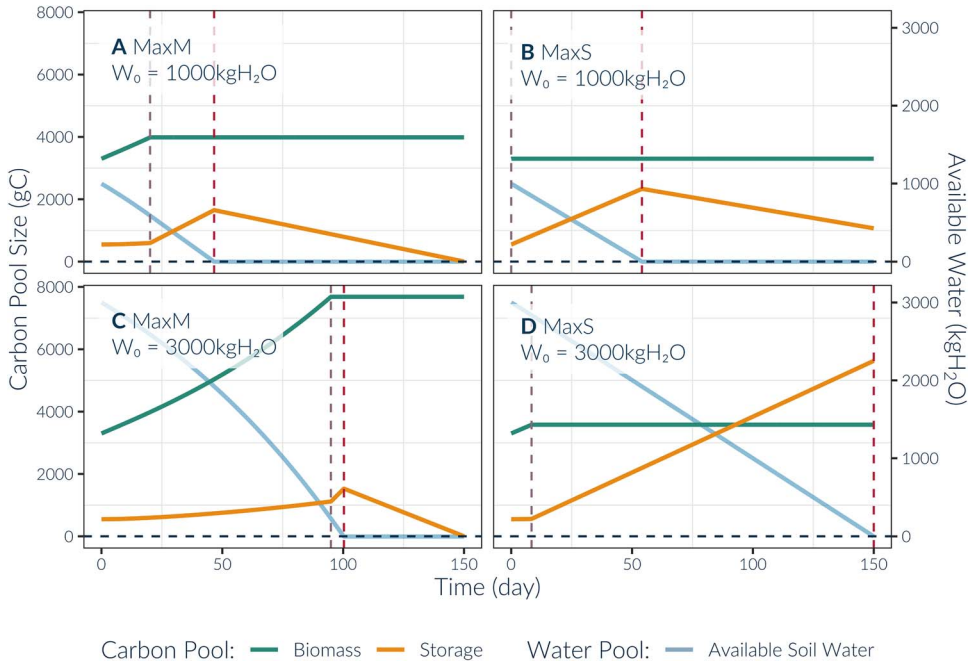

Figure 4. Optimal storage utilization and water pool trajectories for plants under differing goal strategies (maximizing biomass, A and C, and maximizing storage, B and D) and initial water conditions ($W_0 = 1000$ kgH$_2$O, A and B, and $W_0 = 3000$ kgH$_2$O, C and D). Vertical purple dashed lines indicate the optimal switch time, t_s^*, and the red vertical dashed lines indicate the time the water runs out, t_{crit}.

Effect of t_s on the final biomass and storage pool sizes

The time of the switch, t_s, dictates the plant's final biomass pool size, storage pool size, time of water depletion and ultimate survival. A plant which switches off growth earlier has a higher final storage pool but lower final biomass (e.g., $t_s = 10$ days, Figure 3A) compared with a plant that switches later (e.g., $t_s = 20$ days, Figure 3B). On the other hand, switching off growth too late leads to the plant dying (e.g., $t_s = 30$ days, Figure 3C) as the storage pool is insufficient to support respiration through the stress period.

Optimal storage schedule: MaxM and MaxS cases

An optimal value of the time of switch $t_s = t_s^*$ can be found that satisfies the constraints of the model and maximizes the final value of the biomass pool, MaxM, or the storage pool, MaxS (Figure 4). For the MaxM strategy, the optimal schedule involves high values of the optimal time of switch, t_s^*, and fast water depletion. A later allocation switch means there is more time for the plant to accumulate biomass, which increases the risk of storage pool depletion by the end of the simulation. This behaviour is inherent to the optimal solution: if a given switch time has leftover carbon in storage at the end of simulation, this carbon is 'wasted' (in simulation terms) as it could have been allocated to increase growth instead and thus delaying the allocation switch time. Thus, in general, the MaxM strategy has zero storage at the end of the simulation.

Increasing the initial water availability, W_0, leads to a later optimal switch time (e.g., 20.1 days vs 94.9 days for $W_0 = 1000$ kgH$_2$O plant^{-1} and $W_0 = 3000$ kgH$_2$O plant^{-1}) and a significant increase of the final biomass size due to the extended exponential growth. It can also be observed that the optimal storage period decreases with increased initial water availability (Figure 4A and C).

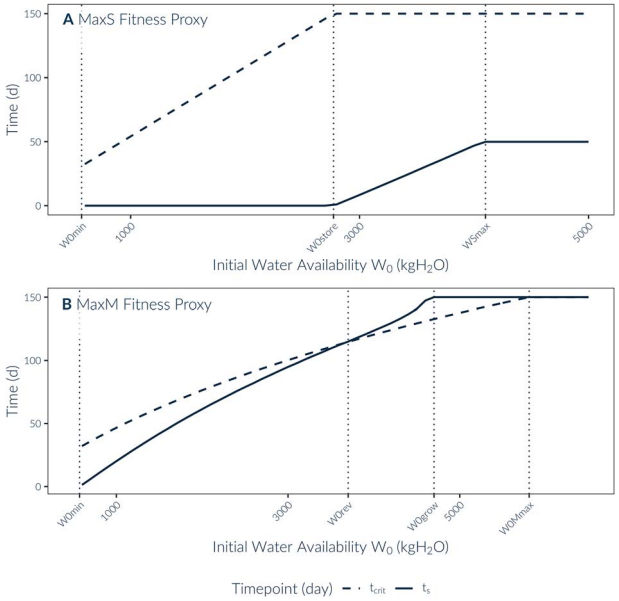

Figure 5. The relationship between the optimal switch time (solid line) and time of water depletion (dashed line) and initial water content for (A) maximizing storage and (B) maximizing biomass. Vertical dotted lines indicate the values of initial water content that demarcate different model behaviours for each strategy. Note that the *x*-axis limits are different between the two plots.

A different optimal behaviour is observed for the MaxS strategy. The growth period is minimized; for lower initial water availabilities, no time is allocated for growing, that is the optimal time of switch from growth to storage is 0: $t^* = 0$ (e.g., Figures 4 and 5B). This implies only a two-phase growth is observed: the plant immediately stops growing, and the two phases involved are storage and stress. Once

Table 2. Description of optimization when optimizing for the MaxM and MaxS goals and changing the initial water pool W_0.

W_0 value	Description
Optimal MaxM behaviour	
$W_0 < W_{0\,min}$	Initial plant water is below the minimum water required for plant survival.
$W_{0\,min} < W_0 < W_{0rev}$	Switch time between growth and storage, t_s, is lower than the time of water depletion, t_{crit}. Both values increase with the growing initial water pool.
$W_{0rev} < W_0 < W_{0grow}$	Time of water depletion, t_{crit}, is lower than time of switch between growth and storage t_s. Both values increase with growing initial water pool.
$W_{0grow} < W_0 < W_{0Mmax}$	Time of water depletion, t_{crit}, is lower than time of switch, t_s; t_s value is at maximum, meaning the plant grows for the entire duration of the drought.
$W_{0Mmax} < W_0$	Time of water depletion, t_{crit} value, reaches the entire duration of the drought period, implying that the plant is no longer droughted. Maximum possible biomass reached.
Optimal MaxS behaviour	
$W_0 < W_{0\,min}$	Initial plant water is below the minimum water required for plant survival.
$W_{0\,min} < W_0 < W_{0store}$	Plant stores for the initial duration of drought (switch time, $t_s = 0$) and time of water depletion, t_{crit}, steadily increases with growing initial water pool.
$W_{0store} < W_0 < W_{0Smax}$	Time of water depletion, t_{crit} value, reaches the entire duration of the drought period, implying that the plant is no longer droughted. Switch time, t_s, increases with growing initial water pool.
$W_{0Smax} < W_0$	Switch time, t_s, reaches maximum possible value and maximum possible storage reached.

water availability becomes high enough, a two-phase growth is observed with the final (stress) phase omitted. The plant first grows and then stores for the rest of the simulation period; water is depleted at the end of the simulation ($t_{crit} = T$; Figure 4D).

Environmental conditions

When the optimal switch time, t_s^*, is used as the 1D proxy for the optimal allocation schedule of individual life strategies, it is possible to find how the initial water availability (W_0) impacts this optimal allocation trajectory (Figure 5). There is a minimum initial water availability, $W_{0\,min}$, that is required for the plant to survive the drought period, given no allocation to biomass (time of switch is 0, leading to no growth phase, $t_s = 0$) and with no stored carbon leftover at the end of the drought period (final value of storage is zero: $S_T = 0$). For the parameter values shown in Table 1, this minimum initial water availability is $W_{0\,min} = 572$ kgH_2O plant^{-1}. For the MaxM strategy, there are five different cases depending on the initial water availability (Table 2). In the first case, initial water availability is smaller than the required minimum ($W_0 < W_{0\,min}$), and the plant cannot survive because the initial water availability is below the minimum required. Therefore, there is no viable optimal schedule. In the second case, the initial water availability is bigger than the minimum and is smaller than the point at which the switch time is at the point of loss of water availability ($W_{0\,min} < W_0 < W_{0rev}$), and a three-phase (growth–storage–stress) growth trajectory is observed: $0 < t_s^* < t_{crit} < T$. In this case, the plant grows for a period and then switches to storing before running out of water and becoming stressed. In the optimal storage schedule, the stored carbon is depleted at the end of the simulation ($S_T = 0$; Figure 5B). The W_{0rev} can be calculated numerically to be $W_{0rev} = 3700$ kgH_2O plant^{-1}. In the third case ($W_{0rev} < W_0 < W_{0growth}$), there is a three-phase growth, but stress and storage switch times are reversed ($t_{crit} < t_s^* < T$) and a phase of growth during stress can be observed. It can also be observed that the stored carbon is still depleted at the end of the simulation ($S_T = 0$; Figure 5B). The $W_{0growth}$ can be calculated numerically to be $W_{0growth} = 4700$ kgH_2O plant^{-1}. The fourth case ($W_{0growth} < W_0 < W_{0Mmax}$) sees the growth period extended over the entirety of the growing period ($t_s^* = T$) and overlapping with the stress period ($t_{crit} < T$). This implies a two-phase growth period: growth and growth during stress with no storage period observed. Additionally, storage is no longer depleted at the end of the simulation ($S_T > 0$).

For the fifth case ($W_0 > W_{0Mmax}$), no more changes in final storage and biomass pools are observed and both time of switch, t_s, and water loss, t_{crit}, are at their maximum, meaning $t_{crit} = t_s^* = T$. This value of W_{0Mmax} can also be found numerically to be $W_{0Mmax} = 5808$ kgH_2O plant^{-1}. The MaxS strategy has four cases (Table 2, Figure 5A). The first case is the same as the MaxM case: $W_0 < W_{0_{min}}$ in which the plant cannot survive because the minimum initial water availability is not sufficient to support the plant for the entirety of the drought period. In the second case ($W_{0_{min}} < W_0 < W_{0store}$, where W_{0store} is the minimum water availability required for a plant to begin to allocate carbon to growth in the MaxS fitness strategy), a two-phase growth is observed with the plant not allocating any carbon to biomass ($t_s^* = 0$) and water is depleted by the end of the simulation ($t_{crit} < T$). The W_{0store} can be found to be $W_{0store} = 2772$ kgH_2O plant^{-1}. The third case ($W_{0store} < W_0 < W_{0Smax}$) has a three-phase growth ($t_s^* > 0$) and the available water is depleted at the end of the simulation ($t_{crit} = T$). In the fourth case ($W_0 > W_{0Smax} = 4075$ kgH_2O plant^{-1}), the plant no longer runs out of water, that is water is available throughout the simulation and at the end of the simulation ($W_T > 0$), and thus it is considered to be not stressed. However, unlike the 'not stressed' case with the MaxM strategy, the plant will still stop growing at some value of $t_s^* < T$ because additional growth might lead to decreased storage. The value of this time of switch, t_s^*, is 49.9 days. However, the benefit of the extra growth at the beginning of the simulation period is small. For water availabilities above W_{0Smax}, when comparing between the optimal trajectory which switches at $t_s^* = 49.9$ days and one that does not grow at all ($t_s^* = 0$ days), there is only an 8% increase in the final storage size.

Fitness strategy and environmental variability

We also explored other intermediate strategies lying between the extreme strategies of MaxM and MaxS. These fitness strategies are specified by the fitness proxy parameter k_f.

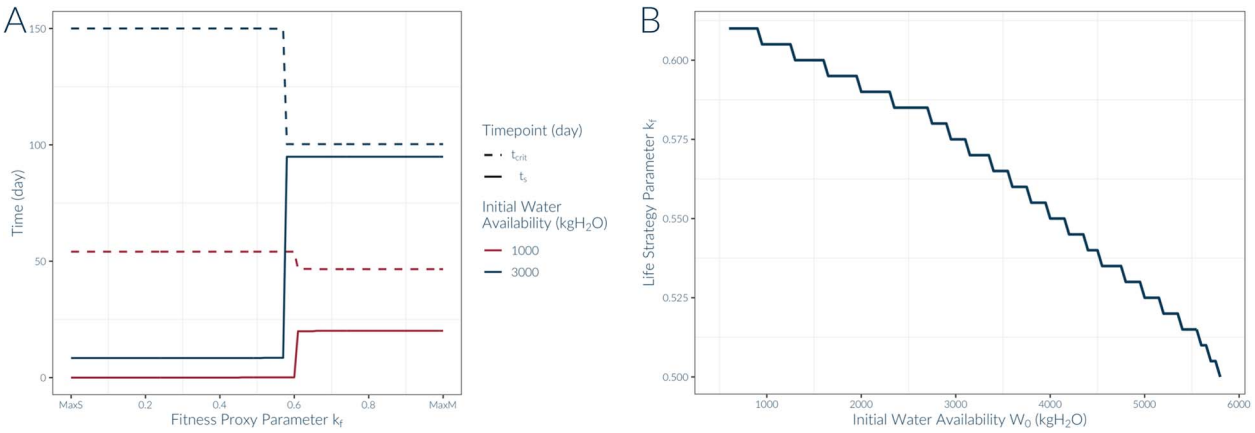

Figure 6. (A) The optimal switch time, t_s^* (solid line), and resulting time of water depletion, t_{crit} (dashed line), for the spectrum of fitness proxy parameters k_f for two initial soil water availabilities: $W_0 = 1000\ kgH_2O$ (red) and $W_0 = 3000\ kgH_2O$ (blue). (B) Point of shift in strategy behaviour between the MaxS safe behaviour (below line) and the MaxM risky behaviour (above line) as determined by the initial water availability. The fitness proxy parameter k_f determines the proportion of biomass versus storage prioritized in the calculation of optimal trajectory. The stepwise discontinuity is an artefact of the resolution of simulation.

The solutions for these intermediate strategies are shown in Figure 6A for two different initial water availabilities ($W_0 = 1000\ kgH_2O\ plant^{-1}$ and $W_0 = 3000\ kgH_2O\ plant^{-1}$). These optimal solutions do not fall on a spectrum but rather follow either the trajectory for the MaxM or the MaxS strategy. This outcome suggests that, although there is a range of theoretical fitness strategies, k_f, there are essentially only two optimal storage schedules: to either allocate as much as possible and deplete the storage ('risky' schedule) or allocate little to biomass and accumulate storage ('safe' schedule).

As the initial water availability increases, the border between the two optimal storage schedules shifts: risky schedules are optimal for a wider range of fitness goals. This outcome is further examined in Figure S1 available as Supplementary data at *Tree Physiology* Online, where the goal function for each fitness proxy parameter value, Φ_{kf}, are presented for a range of switch time values. The pool sizes either increase with the lengthened growing time or decrease depending on the proportion of final storage and biomass size in the final carbon outputs. For larger values of initial water availability, W_0, the size increases first peaked at the MaxS optimal switch time t_s^*. Later, the size decreased for strategies that followed MaxS and increased for strategies that followed MaxM behaviour.

These trends are consistent for the entire spectrum of initial water availability W_0 values that encompass the drought conditions and it can be further seen that the border between the two alternative strategies decreases with higher W_0 but stays within the range of $0.5 < k_f < 0.7$ (Figure 6B).

Discussion

The key outcome of our optimization model analysis is that the optimal growth strategy during a drought is a three-phase trajectory: (i) an initial period, when soil moisture is high, when growth occurs at the maximum rate, increasing growth and future carbon gain; (ii) an intermediate period, when carbon is stored and no growth occurs; and (iii) finally, the stress period, when both photosynthesis and growth are zero and stored carbon is used for maintenance respiration. While some alternative optimal growth strategies emerged, these are generally simplifications that exclude one of the three phases, and the optimal pattern remains consistent for a wide range of initial water conditions and fitness proxies. Crucially, in almost all cases, the optimal point for growth to stop occurs before the plant is fully stressed, leading to storage accumulation, irrespective of the objective function being maximized. This behaviour, often observed in droughted plants (Würth et al. 2005, Adams 2013, Duan et al. 2013, Mitchell et al. 2014), has been commonly associated with sink limitation and passive NSC storage (Muller et al. 2011, Palacio et al. 2014, Körner 2015, 2020, Zweifel et al. 2021). However, our results indicate that this behaviour would also be expected under the active storage hypothesis. Wiley and Helliker (2012) argued that plants may have adapted to avoid carbon depletion during stress by accumulating carbon during the initial phase of stress which, as our results suggest, requires growth to halt before photosynthesis. Here, our results demonstrate the hypothetical trajectory of active storage when modelling the process of carbon storage under stress.

The tendency for NSC content to increase at the onset of drought before later decreasing can thus be consistent with of active storage allocation strategy. However, the adoption of different strategies (MaxS and MaxM) results in different NSC dynamics and may hint at links to species-specific strategies and relationships to drought tolerance. For example, Mitchell et al. (2014) showed that after subjecting *Eucalyptus globulus* seedlings to drought, plants first slowed growth, then accumulated NSCs until photosynthesis stopped. In the same experiment, *Pinus radiata* seedlings grew for a longer time and accumulated much less NSCs before photosynthesis ceased. The difference in response between the two species emulate the two MaxS (*E. globulus*) and MaxM (*P. radiata*) survival strategies in the face of stress. The *E. globulus* has adapted both to drought (Valdés et al. 2013) and fire (Catry et al. 2013), resprouting following stem mortality. These adaptations may require *E. globulus* to maintain higher NSC stores. By contrast, *P. radiata* occurs naturally in a small area, is less drought adapted than other gymnosperms (Duan et al. 2015), and while being relatively fire resistant, it relies on seed germination as a response to fire and cannot resprout post-fire (Fernandes et al. 2008). Another important difference between the two species' responses is the turgor loss point: the leaf water potential at which wilting is observed is a

measurement that positively correlated with drought tolerance (Zhu et al. 2018), and maintaining cell turgor is required for cell division and growth (Tardieu et al. 2011). If active storage is observed, it would suggest that plants stop growing before the soil water potential reaches the species' turgor loss point. Indeed, the difference between species turgor loss points (−2.03 MPa in *E. globulus* and −1.41 MPa in *P. radiata*) and the water potential at which the individuals stopped growing (∼−1.4 MPa) suggested that only *P. radiata* had a physical water-stress limitation. This observation suggests that the *P. radiata* prioritizes growth over storage during stress by extending growth to its physiological limit, as predicted by the optimization for the MaxM strategy.

Other comparative drought studies in plants also show differences in timing or magnitude of growth and NSC accumulation. For example, a study of seasonal drought in nut trees showed a large NSC seasonality and a peak in NSC concentration following the cessation of growth in almond, but a smaller response in walnut and pistachio, with NSC concentrations remaining fairly stable throughout the year (Tixier et al. 2020). Similarly, provenance may also play a role: e.g., *Phacelia secunda* individuals from temperature-limited environments prioritize carbon allocation to storage more than those from water-limited environments (Reyes-Bahamonde et al. 2021).

The distinct pattern resulting from the model analysis, growth–storage–stress, can significantly aid in understanding the dynamics of active carbon storage allocation in the field. The time between the cessation of growth, t_s, and the cessation of photosynthesis, t_{crit}, is referred to in physiological literature as the Carbon Safety Margin (Mitchell et al. 2014). In the results of the optimization, the two strategies showed significant differences in the length of the Carbon Safety Margin: MaxM minimized this period, while MaxS maximized it, thus hinting at the potential link of the strategy to drought tolerance and alternative carbon storage strategies. Notably, one does not need destructive sampling to identify these time points: cessation of growth and cessation of photosynthesis can be observed and measured in vivo using standard growth and gas exchange measurements. If the link between these time points and peak NSC and stress-inducing water potential can be further supported through integration of optimization modelling into experimental work, we can attempt to infer storage dynamics from proxy observation and gain insight about the process in a wider range of species and scenarios.

Our simple model makes several unrealistic simplifications for the sake of analytical tractability. For example, photosynthesis is assumed not to slow during drought and only to stop when the soil moisture is fully depleted. While we do not believe these simplifications affect the fundamental conclusion of our study, further insights could potentially be obtained by implementing more realistic stomatal and hydraulic behaviour in the model. For example, adding stomatal and hydraulic function would allow the exploration of the relationship between the carbon safety margin and the hydraulic safety margin (Meir et al. 2015), which is generally defined as the degree of conservatism in a plant hydraulic strategies and expressed as, for example, the difference between the minimum xylem pressure a stem experiences and the pressure at which it would lose 50% of its hydraulic conductivity (Johnson et al. 2012). The hydraulic safety margin is thought to be a good predictor for plant mortality during drought (Anderegg et al. 2016), and it has increasingly been used in optimality models that predict stomatal and photosynthetic responses to drought (e.g., Anderegg et al. 2018, Mrad et al. 2019). Linking the two optimizations would be a promising avenue to understand plant responses to drought stress more fully.

Other elaborations of the model would also be of interest to explore. For example, one important simplification in the model is the 'bucket' representation of the soil water availability, which assumes a fixed amount of water available to the plant. The model could potentially be extended to enable the available soil moisture to increase with the growing root biomass. Adding this feature to the model would alter the trade-off towards growth, particularly of root biomass, and could potentially alter the outcome of the optimal storage strategy. Similarly, we have assumed that plant respiration rates are constant and that turnover does not occur. Respiration rates may decline under stress (Ayub et al. 2011), which would alter the growth/storage trade-off by reducing the requirement for NSC storage. Turnover is also likely to occur during drought. Dropping of leaves and branches is a common plant strategy which would affect the growth/storage trade-off by lowering costs during stress, but decreasing plant competitive ability after the stress is alleviated. Additionally, there is evidence that when plants are stressed, they become more susceptible to pathogens and herbivory; investment in defence is then crucial to avoid mortality, giving rise to a growth–defence trade-off (Deslauriers et al. 2015, Monson et al. 2021). An elaboration of the model could potentially explore relative allocation to growth, defence and storage.

The ecological context for our model is also important. We consider a situation in which plants are competing for resources but are subject to a periodic drought, such as a productive temperate or tropical forest with a predictable dry season. Other ecological contexts could have similar growth/storage trade-offs, such as boreal forests with a cold stress period, or forests with regular fire return intervals. However, the trade-off is not likely to be universally applicable; for example, it may not apply in desert environments, where plant–plant competition for resources is limited.

Finally, we have assumed a constant drought duration in our model, whereas most droughts are unpredictable in length. A stochastic version of the OCT approach used here has previously been successfully applied to predict some aspects of plant function during drought (Cowan 1986, Mäkelä et al. 1996, Lu et al. 2019) and could potentially be applied here. However, it is not clear that extending the optimization in this direction would provide more insight, in particular because of the need to consider plant mortality when there is insufficient allocation to storage. In future work, we aim to embed the results of the current study in a long-term dynamic model that directly simulates competition among species with different fitness maximization strategies (Stefaniak 2021).

In conclusion, we have shown that a modelled optimal carbon storage allocation trajectory can explain some of the observed patterns of carbon storage dynamics in response to water stress. Our results indicate that the cessation of growth before photosynthesis can be interpreted as an active storage response rather than a purely passive outcome of physiological growth limitation. The use of phenological observations, such as growth cessation or NSC maxima during stress, may help to explain the observed variability in drought tolerance and allocation strategies of different species and to understand

the role of carbon storage and the mechanisms for carbon allocation.

Authors' contributions

E.Z.S., D.T.T., R.C.D. and B.E.M. designed the experiment. E.Z.S. conducted the modelling and data analyses, and wrote the paper, with contributions from D.T.T., R.C.D. and B.E.M. All authors edited and approved the final manuscript.

Supplementary data

Supplementary data for this article are available at *Tree Physiology* Online.

Funding

This work was supported by Australian Research Council Discovery Grant DP160103436.

Conflict of interest

None declared.

Data availability

The code is freely available at https://github.com/foxeswithdata/StoringForDrought.

References

Adams HD, Zeppel MJB, Anderegg WRL et al. (2017) A multi-species synthesis of physiological mechanisms in drought-induced tree mortality. Nat Ecol Evol 1:1285–1291. https://doi.org/10.1038/s41559-017-0248-x.

Adams MA (2013) Mega-fires, tipping points and ecosystem services: managing forests and woodlands in an uncertain future. For Ecol Manage 294:250–261. https://doi.org/10.1016/j.foreco.2012.11.039.

Anderegg WRL, Klein T, Bartlett M, Sack L, Pellegrini AFA, Choat B, Jansen S (2016) Meta-analysis reveals that hydraulic traits explain cross-species patterns of drought-induced tree mortality across the globe. Proc Natl Acad Sci USA 113:5024–5029. https://doi.org/10.1073/pnas.1525678113.

Anderegg WRL, Wolf A, Arango-Velez A et al. (2018) Woody plants optimise stomatal behaviour relative to hydraulic risk. Ecol Lett 21:968–977. https://doi.org/10.1111/ele.12962.

Atkinson RRL, Burrell MM, Rose KE, Osborne CP, Rees M (2014) The dynamics of recovery and growth: how defoliation affects stored resources. Proc R Soc B Biol Sci 281:20133355. https://doi.org/10.1098/rspb.2013.3355.

Ayub G, Smith RA, Tissue DT, Atkin OK (2011) Impacts of drought on leaf respiration in darkness and light in *Eucalyptus saligna* exposed to industrial-age atmospheric CO_2 and growth temperature. New Phytol 190:1003–1018. https://doi.org/10.1111/j.1469-8137.2011.03673.x.

Bierhuizen JF, Slatyer RO (1965) Effect of atmospheric concentration of water vapour and CO2 in determining transpiration-photosynthesis relationships of cotton leaves. Agric Meteorol 2:259–270. https://doi.org/10.1016/0002-1571(65)90012-9.

Blackman CJ (2018) Leaf turgor loss as a predictor of plant drought response strategies. Tree Physiol 38:655–657. https://doi.org/10.1093/treephys/tpy047.

Bloom AJ, Chapin FS III, Mooney HA (1985) Resource limitation in plants—an economic analogy. Annu Rev Ecol Syst 16:363–392. https://doi.org/10.1146/annurev.es.16.110185.002051.

Blumenthal DM, Mueller KE, Kray JA, Ocheltree TW, Augustine DJ, Wilcox KR (2020) Traits link drought resistance with herbivore defence and plant economics in semi-arid grasslands: the central roles of phenology and leaf dry matter content. J Ecol 108:2336–2351. https://doi.org/10.1111/1365-2745.13454.

Boltyanskii VG, Gamkrelidze RV, Pontryagin LS (1960) The theory of optimal processes. I. The maximum principle. Los Aangeles (CAL): TRW Space Technology Labs.

Boyer JS (2018) Plant water relations: a whirlwind of change. In: Cánovas FM, Lüttge U, Matyssek R (eds) Progress in botany, Vol. 79. Springer International Publishing, pp 1–31. https://doi.org/10e.1007/124_2017_3.

Cabon A, Kannenberg SA, Arain A et al. (2022) Cross-biome synthesis of source versus sink limits to tree growth. Science 376:758–761. https://doi.org/10.1126/science.abm4875.

Catry FX, Moreira F, Tujeira R, Silva JS (2013) Post-fire survival and regeneration of *Eucalyptus globulus* in forest plantations in Portugal. For Ecol Manage 310:194–203. https://doi.org/10.1016/j.foreco.2013.08.036.

Chiariello N, Roughgarden J (1984) Storage allocation in seasonal races of an annual plant: optimal versus actual allocation. Ecology 65:1290–1301. https://doi.org/10.2307/1938334.

Chuste P-A, Maillard P, Bréda N, Levillain J, Thirion E, Wortemann R, Massonnet C (2020) Sacrificing growth and maintaining a dynamic carbohydrate storage are key processes for promoting beech survival under prolonged drought conditions. Trees 34:381–394. https://doi.org/10.1007/s00468-019-01923-5.

Clark JS, Dietze M, Chakraborty S, Agarwal PK, Ibanez I, LaDeau S, Wolosin M (2007) Resolving the biodiversity paradox. Ecol Lett 10:647–659. https://doi.org/10.1111/j.1461-0248.2007.01041.x.

Cowan I, Farquhar GD (1977) Stomatal function in relation to leaf metabolism and environment. In: Integration of activity in the higher plant. Cambridge: Cambridge University Press, pp 471–505.

Cowan, IR (1986) Economics of carbon fixation in higher plants. Economics of carbon fixation in higher. plants 133–170.

Deslauriers A, Caron L, Rossi S (2015) Carbon allocation during defoliation: testing a defense-growth trade-off in balsam fir. Front Plant Sci 6. https://doi.org/10.3389/fpls.2015.00338.

Dietze MC, Sala A, Carbone MS, Czimczik CI, Mantooth JA, Richardson AD, Vargas R (2014) Nonstructural carbon in woody plants. Annu Rev Plant Biol 65:667–687. https://doi.org/10.1146/annurev-arplant-050213-040054.

Drake JE, Tjoelker MG, Aspinwall MJ, Reich PB, Pfautsch S, Barton CVM (2019) The partitioning of gross primary production for young *Eucalyptus tereticornis* trees under experimental warming and altered water availability. New Phytol 222:1298–1312. https://doi.org/10.1111/nph.15629.

Duan H, Amthor JS, Duursma RA, O'Grady AP, Choat B, Tissue DT (2013) Carbon dynamics of eucalypt seedlings exposed to progressive drought in elevated [CO^2] and elevated temperature. Tree Physiol 33:779–792. https://doi.org/10.1093/treephys/tpt061.

Duan H, O'Grady AP, Duursma RA, Choat B, Huang G, Smith RA, Jiang Y, Tissue DT (2015) Drought responses of two gymnosperm species with contrasting stomatal regulation strategies under elevated [CO_2] and temperature. Tree Physiol 35:756–770. https://doi.org/10.1093/treephys/tpv047.

Eller CB, Barros FDV, Bittencourt PRL, Rowland L, Mencuccini M, Oliveira RS (2018) Xylem hydraulic safety and construction costs determine tropical tree growth: tree growth vs hydraulic safety trade-off. Plant Cell Environ 41:548–562. https://doi.org/10.1111/pce.13106.

Fatichi S, Pappas C, Zscheischler J, Leuzinger S (2019) Modelling carbon sources and sinks in terrestrial vegetation. New Phytol 221:652–668. https://doi.org/10.1111/nph.15451.

Fernandes PM, Vega JA, Jiménez E, Rigolot E (2008) Fire resistance of European pines. For Ecol Manage 256:246–255. https://doi.org/10.1016/j.foreco.2008.04.032.

Ferner E, Rennenberg H, Kreuzwieser J (2012) Effect of flooding on C metabolism of flood-tolerant (*Quercus robur*) and non-tolerant

(*Fagus sylvatica*) tree species. Tree Physiol 32:135–145. https://doi.org/10.1093/treephys/tps009.
Franklin O (2007) Optimal nitrogen allocation controls tree responses to elevated CO_2. New Phytol 174:811–822. https://doi.org/10.1111/j.1469-8137.2007.02063.x.
Franklin O, Johansson J, Dewar RC, Dieckmann U, McMurtrie RE, Brannstrom A, Dybzinski R (2012) Modeling carbon allocation in trees: a search for principles. Tree Physiol 32:648–666. https://doi.org/10.1093/treephys/tpr138.
Hartmann H, Trumbore S (2016) Understanding the roles of nonstructural carbohydrates in forest trees – from what we can measure to what we want to know. New Phytol 211:386–403. https://doi.org/10.1111/nph.13955.
Hilbert DW (1990) Optimization of plant root: shoot ratios and internal nitrogen concentration. Ann Bot 66:91–99. https://doi.org/10.1093/oxfordjournals.aob.a088005.
Iwasa Y, Cohen D (1989) Optimal growth schedule of a perennial plant. Am Nat 133:480–505.
Iwasa Y, Roughgarden J (1984) Shoot/root balance of plants: optimal growth of a system with many vegetative organs. Theor Popul Biol 25:78–105. https://doi.org/10.1016/0040-5809(84)90007-8.
Johnson DM, McCulloh KA, Woodruff DR, Meinzer FC (2012) Hydraulic safety margins and embolism reversal in stems and leaves: Why are conifers and angiosperms so different? Plant Sci 195:48–53. https://doi.org/10.1016/j.plantsci.2012.06.010.
Kaelke CM, Kruger EL, Reich PB (2001) Trade-offs in seedling survival, growth, and physiology among hardwood species of contrasting successional status along a light-availability gradient. Can J For Res 31:1602–1616. https://doi.org/10.1139/x01-090.
Körner C (2015) Paradigm shift in plant growth control. Curr Opin Plant Biol 25:107–114. https://doi.org/10.1016/j.pbi.2015.05.003.
Körner C (2020) Tools shape paradigms of plant-environment interactions. In: Cánovas FM, Lüttge U, Risueño M-C, Pretzsch H (eds) Progress in botany, Vol. 82. Springer International Publishing, pp 1–41. https://doi.org/10.1007/124_2020_41.
Kozlowski TT (1992) Carbohydrate sources and sinks in woody plants. Bot Rev 58:107–222. https://doi.org/10.1007/BF02858600.
Kreuzwieser J, Rennenberg H (2014) Molecular and physiological responses of trees to waterlogging stress: responses of tree to waterlogging. Plant Cell Environ 37:2245–2259. https://doi.org/10.1111/pce.12310.
Lenhart S, Workman JT (2007) Optimal control applied to biological models. New York (NY): Chapman and Hall/CRC. https://doi.org/10.1201/9781420011418.
Lerdau M (1992) Future discounts and resource allocation in plants. Funct Ecol 6:371. https://doi.org/10.2307/2389273.
Lu Y, Duursma RA, Medlyn BE (2016) Optimal stomatal behaviour under stochastic rainfall. J Theor Biol 394:160–171. https://doi.org/10.1016/j.jtbi.2016.01.003.
Lu Y, Duursma RA, Farrior CE, Medlyn BE, Feng X (2019) Optimal stomatal drought response shaped by competition for water and hydraulic risk can explain plant trait covariation. New Phytologist. Portico. 225(3):1206–1217. https://doi.org/10.1111/nph.16207.
Mäkelä A, Berninger F, Hari P (1996) Optimal Control of Gas Exchange during Drought: theoretical analysis. Annals of Botany 77(5):461–468. https://doi.org/10.1006/anbo.1996.0056.
McDowell N, Pockman WT, Allen CD et al. (2008) Mechanisms of plant survival and mortality during drought: Why do some plants survive while others succumb to drought? New Phytol 178:719–739. https://doi.org/10.1111/j.1469-8137.2008.02436.x.
McDowell NG, Sapes G, Pivovaroff A et al. (2022) Mechanisms of woody-plant mortality under rising drought, CO2 and vapour pressure deficit. Nat Rev Earth Environ 3:5. https://doi.org/10.1038/s43017-022-00272-1.
McMurtrie RE, Dewar RC (2013) New insights into carbon allocation by trees from the hypothesis that annual wood production is maximized. New Phytol 199:981–990. https://doi.org/10.1111/nph.12344.
Medlyn BE, Duursma RA, Eamus D et al. (2011) Reconciling the optimal and empirical approaches to modelling stomatal conductance. Glob Chang Biol 17:2134–2144. https://doi.org/10.1111/j.1365-2486.2010.02375.x.
Meir P, Mencuccini M, Dewar RC (2015) Drought-related tree mortality: addressing the gaps in understanding and prediction. New Phytol 207:28–33. https://doi.org/10.1111/nph.13382.
Mitchell PJ, O'Grady AP, Tissue DT, Worledge D, Pinkard EA (2014) Co-ordination of growth, gas exchange and hydraulics define the carbon safety margin in tree species with contrasting drought strategies. Tree Physiol 34:443–458. https://doi.org/10.1093/treephys/tpu014.
Moeller HV, Neubert MG (2016) Multiple friends with benefits: An optimal mutualist management strategy? Am Nat 187:E1–E12. https://doi.org/10.1086/684103.
Monson RK, Trowbridge AM, Lindroth RL, Lerdau MT (2021) Coordinated resource allocation to plant growth–defense tradeoffs. New Phytol 233:1051–1066. https://doi.org/10.1111/nph.17773.
Mori S, Yamaji K, Ishida A et al. (2010) Mixed-power scaling of whole-plant respiration from seedlings to giant trees. Proc Natl Acad Sci USA 107:1447–1451. https://doi.org/10.1073/pnas.0902554107.
Mrad A, Sevanto S, Domec J-C, Liu Y, Nakad M, Katul G (2019) A dynamic optimality principle for water use strategies explains isohydric to anisohydric plant responses to drought. Front For Glob Change 2:49. https://doi.org/10.3389/ffgc.2019.00049.
Muller B, Pantin F, Génard M, Turc O, Freixes S, Piques M, Gibon Y (2011) Water deficits uncouple growth from photosynthesis, increase C content, and modify the relationships between C and growth in sink organs. J Exp Bot 62:1715–1729. https://doi.org/10.1093/jxb/erq438.
O'Brien MJ, Leuzinger S, Philipson CD, Tay J, Hector A (2014) Drought survival of tropical tree seedlings enhanced by non-structural carbohydrate levels. Nat Clim Change 4:710–714. https://doi.org/10.1038/nclimate2281.
Onoda Y, Wright IJ, Evans JR, Hikosaka K, Kitajima K, Niinemets Ü, Poorter H, Tosens T, Westoby M (2017) Physiological and structural tradeoffs underlying the leaf economics spectrum. New Phytol 214:1447–1463. https://doi.org/10.1111/nph.14496.
Palacio S, Hoch G, Sala A, Körner C, Millard P (2014) Does carbon storage limit tree growth? New Phytol 201:1096–1100. https://doi.org/10.1111/nph.12602.
Parker GA, Smith JM (1990) Optimality theory in evolutionary biology. Nature 348:27–33. https://doi.org/10.1038/348027a0.
Piper FI, Moreno-Meynard P, Fajardo A (2022) Nonstructural carbohydrates predict survival in saplings of temperate trees under carbon stress. Funct Ecol 36:2806–2818. https://doi.org/10.1111/1365-2435.14158.
Poorter L, Kitajima K (2007) Carbohydrate storage and light requirements of tropical moist and dry forest tree species. Ecology 88:1000–1011. https://doi.org/10.1890/06-0984.
Potkay A, Hölttä T, Trugman AT, Fan Y (2021*a*) Turgor-limited predictions of tree growth, height, and metabolic scaling over tree lifespans. Tree Physiol 42:229–252. https://doi.org/10.1093/treephys/tpab094.
Potkay A, Trugman AT, Wang Y, Venturas MD, Anderegg WRL, Mattos CRC, Fan Y (2021*b*) Coupled whole-tree optimality and xylem hydraulics explain dynamic biomass partitioning. New Phytol 230:2226–2245. https://doi.org/10.1111/nph.17242.
Reed CC, Hood SM (2023) Nonstructural carbohydrates explain post-fire tree mortality and recovery patterns. Tree Physiol 44:tpad155. https://doi.org/10.1093/treephys/tpad155.
Reyes-Bahamonde C, Piper FI, Cavieres LA (2021) Carbon allocation to growth and storage depends on elevation provenance in an herbaceous alpine plant of Mediterranean climate. Oecologia 195:299–312. https://doi.org/10.1007/s00442-020-04839-x.
Ruehr NK, Grote R, Mayr S, Arneth A (2019) Beyond the extreme: recovery of carbon and water relations in woody plants following heat and drought stress. Tree Physiol 39:1285–1299. https://doi.org/10.1093/treephys/tpz032.

Rüger N, Condit R, Dent DH, DeWalt SJ, Hubbell SP, Lichstein JW, Lopez OR, Wirth C, Farrior CE (2020) Demographic trade-offs predict tropical forest dynamics. Science 368:165–168. https://doi.org/10.1126/science.aaz4797.

Sinclair TR, Tanner CB, Bennett JM (1984) Water-use efficiency in crop production. Bioscience 34:36–40. https://doi.org/10.2307/1309424.

Stearns SC (1989) Trade-offs in life-history evolution. Funct Ecol 3:259. https://doi.org/10.2307/2389364.

Stefaniak EZ (2021) Modelling optimal plant carbon storage [Ph.D. thesis]. Penrith (NSW): Western Sydney University. http://hdl.handle.net/1959.7/uws:68787.

Stengel RF (2012) Optimal control and estimation. 2nd ed. New York (NY): Dover Publications.

Tardieu F, Granier C, Muller B (2011) Water deficit and growth. Coordinating processes without an orchestrator? Curr Opin Plant Biol 14:283–289. https://doi.org/10.1016/j.pbi.2011.02.002.

Tixier A, Guzmán-Delgado P, Sperling O, Amico Roxas A, Laca E, Zwieniecki MA (2020) Comparison of phenological traits, growth patterns, and seasonal dynamics of non-structural carbohydrate in Mediterranean tree crop species. Sci Rep 10:347. https://doi.org/10.1038/s41598-019-57016-3.

Valdés AE, Irar S, Majada JP, Rodríguez A, Fernández B, Pagès M (2013) Drought tolerance acquisition in *Eucalyptus globulus* (Labill.): a research on plant morphology, physiology and proteomics. J Proteomics 79:263–276. https://doi.org/10.1016/j.jprot.2012.12.019.

Wiley E, Helliker B (2012) A re-evaluation of carbon storage in trees lends greater support for carbon limitation to growth. New Phytol 195:285–289. https://doi.org/10.1111/j.1469-8137.2012.04180.x.

Wolf A, Anderegg WRL, Pacala SW (2016) Optimal stomatal behavior with competition for water and risk of hydraulic impairment. Proc Natl Acad Sci USA 113:E7222–E7230. https://doi.org/10.1073/pnas.1615144113.

Wright IJ, Reich PB, Westoby M et al. (2004) The worldwide leaf economics spectrum. Nature 428:821–827. https://doi.org/10.1038/nature02403.

Würth MKR, Peláez-Riedl S, Wright SJ, Körner C (2005) Non-structural carbohydrate pools in a tropical forest. Oecologia 143:11–24. https://doi.org/10.1007/s00442-004-1773-2.

Zhu S-D, Chen Y-J, Ye Q, He P-C, Liu H, Li R-H, Fu P-L, Jiang G-F, Cao K-F (2018) Leaf turgor loss point is correlated with drought tolerance and leaf carbon economics traits. Tree Physiol 38:658–663. https://doi.org/10.1093/treephys/tpy013.

Zweifel R, Sterck F, Braun S et al. (2021) Why trees grow at night. New Phytol 231:2174–2185. https://doi.org/10.1111/nph.17552.

Tree Physiology, 2024, 44, 34–45
https://doi.org/10.1093/treephys/tpae032
Research paper